in the crystal lattice. The molecules of **1** occupy a site of crystallographic inversion symmetry. The porphyrin ligand is centrosymmetric, so the four porphyrin nitrogens are rigorously coplanar. The Mn≡N moiety is statistically disordered about the inversion center with the Mn → N vector approximately normal to the N_4 plane as shown in the ORTEP diagram (Figure 1). The porphyrin core is remarkably planar with no deviations of the core atoms of more than 0.06 Å from the N_4 plane. The Mn atom is 0.388 Å out of the N_4 plane. The critical distances (Å) are as follows: Mn–N1 = 2.022 (2), Mn–N1′ = 2.021 (2), Mn–N2 = 1.983 (2), Mn–N2′ = 2.060 (2), Mn–N3(nitride) = 1.515 (3) Å. This Mn≡N(nitride) bond distance is the same as that found in the porphodimethenenitridomanganese(V) structure (1.512 (2) Å)[8] and is shorter than all other Mn≡N bonds reported in the literature.

Gel permeation chromatography (THF–BioBeads S-X3) establishes that **1** and the more soluble complex, $NMn^{V}TpTP$, are monomeric in solution. The infrared spectrum of $NMn^{V}TPP$ displays a band at 1036 cm^{-1} for the Mn≡N stretching fundamental that shifts to a shoulder at 1008 cm^{-1} upon substitution with ^{15}N. Absent in the infrared spectra of the nitride complexes are any characteristic porphyrin π-cation radical bands ($TPP^{\cdot+}$) at 1270–1290 cm^{-1}.[13] The ^1H NMR line widths and chemical shifts of **1** and $NMn^{V}TpTP$ establish that the nitride complexes are diamagnetic.[14] All the above evidence is in accord with a low-spin d^2 Mn(V) neutral porphyrin ground electronic state for these nitride complexes.

The quantitative electronic specrum of $NMn^{V}TPP$, compared with representative $Mn^{IV}TPP$ and $Mn^{III}TPP$ complexes in Figure 2, is a classical "normal" metalloporphyrin spectrum.[15] The principal bands in the visible spectrum, the B or Soret band (λ_{max} 424 nm) and the Q band (λ_{max} 538 nm) are π,π* in origin and minimally perturbed by high-energy $a_{1u}(\pi),a_{2u}(\pi) \rightarrow e_g(d_\pi)$ charge-transfer (CT) transitions. The published visible spectra of the isoelectronic $O{=}Cr^{IV}TPP$ complex[16,17] shows similar but broader bands than $NMn^{V}TPP$, in agreement with a greater but still limited perturbation of the π,π* bands by high-energy CT transitions in the former relative to the latter. One would also expect a greater disruption of the porphyrin-ligand-based molecular orbitals and the widths and intensities of the characteristic π,π* bands in the $O{=}Cr^{IV}TPP$ complex than in the nitride complexes, for the X-ray structure of the former[16] shows a domed porphyrin ligand and not a flat porphyrin ligand as in **1**.

Complex **1** is more thermally stable than the other high-valent Mn porphyrins previously isolated and characterized and can be recovered intact after 2 min in refluxing chlorobenzene (bp = 132 °C). When **1** is treated with ≥1 equiv of a strong mineral acid, e.g., triflic acid, in aprotic media, e.g., chlorobenzene or dichloromethane, it decomposes rapidly to the $[Mn^{III}TPP]^+$ chromophore. The complex does not react under neutral or acidic conditions to transfer its nitride nitrogen to alkanes or alkenes. The low reactivity and high formal oxidation state[18] of **1** argue for the importance of diradical and paramagnetic ground electronic states in the high-valent Mn species responsible for attack on unactivated hydrocarbons in the Mn porphyrin based oxidation systems.[3,4]

Acknowledgment. Support of this work by the National Science Foundation (Grant No. CHE-7909730 and by the donors of the Petroleum Research Fund, administered by the American Chemical Society (ACS-PRF grant No. 12486-AC4), is acknowledged.

Registry No. 1·*n*-C_6H_5Cl, 83632-53-5; $NMn^{V}TPP$, 83632-54-6; $[N_3Mn^{IV}TPP]_2O$, 79775-62-5; $ClMn^{III}TPP$, 32195-55-4.

Supplementary Material Available: Tables of atomic positional and thermal parameters, bond distances and angles, and an ORTEP diagram displaying the atom numbering scheme (6 pages). Ordering information is given on any current masthead page.

(12) The structure was solved at the U.C. Berkeley X-ray Crystallographic Facility (CHEXRAY) by a combination of vector methods, direct methods, and brute force. Equipment at CHEXRAY and general refinement procedures used may be found in ref 6 and 7.

(13) Shimomura, E. T.; Phillippi, M. A.; Goff, H. M.; Scholz, W. F.; Reed, C. A. *J. Am. Chem. Soc.* **1981**, *103*, 6778–6780.

(14) The ^1H NMR chemical shifts for **1** at 20 °C ($CDCl_3$) are as follows: δ 4.04 (s, 12 H, CH_3O), 7.23 (d. 8 H, *m*-PhH), 8.04, (d, 8 H, *o*-PhH), 8.93 (s, 8 H, β-pyrrole H). At this temperature the phenyl groups are freely rotating on the NMR time scale, and the doublets arise from the coupling of adjacent *o*-PhH and *m*-PhH protons.

(15) Gouterman, M. In "The Porphyrins"; Dolphin, D., Ed.; Academic Press: New York, 1978; Vol. III, Chapter 1.

(16) Groves, J. T.; Kruper, W. J., Jr.; Haushalter, R. C.; Butler, W. M. *Inorg. Chem.* **1982**, *21*, 1363–1368.

(17) Buchler, J. W.; Lay, K. L.; Castle, L. Ullrich, V. *Inorg. Chem.* **1982**, *21*, 842–844.

(18) ESCA measurements on **1** and several $Mn^{IV}TPP$ and $Mn^{III}TPP$ complexes also indicate that the effective atomic charge on Mn in the nitride complexes is higher than in all the other MnTPP species: Eyermann, J.; Jolly, W. L.; Schardt, B. C.; Smegal, J. A.; Camenzind, M. J.; Hill, C. L., unpublished work.

Talaromycins: Application of Homonuclear Spin Correlation Maps to Structure Assignment

David G. Lynn,* Nancy J. Phillips, William C. Hutton, and Jeffrey Shabanowitz

Department of Chemistry, University of Virginia Charlottesville, Virginia 22901

D. I. Fennell and R. J. Cole

National Peanut Research Laboratory Dawson, Georgia 31742

Received May 28, 1982

Poultry house litter, which may consist of sawdust, wood shavings, or peanut hulls with accumulated chicken manure, feathers, and wasted food, has been successfully used as a part of livestock diet.[1,2] A toxicogenic fungus identified as *Talaromyces stipitatus* has been isolated from a wood-shavings-based chicken litter.[3] The culturing of this fungus has allowed for the isolation of the toxic metabolite. We describe the application of proton homonuclear correlation spectroscopy (COSY) to the structure assignment of this metabolite.

Cultures of *T. stipitatus* in 45 Fernback flasks (2.8 L) each containing 200 mL of mycological broth (Difco Laboratories) at pH 4.8 supplemented with 15% sucrose and 2% yeast extract were kept at 27 °C for 18 days. The cultures were homogenized and filtered through cheesecloth, and the filtrate was extracted with $CHCl_3$. This dried organic layer was applied directly to silica gel (9.5 × 17 cm) and sequentially eluted with hexanes, benzene, ethyl ether, chloroform, ethyl acetate, and acetone. The active[3] ethyl acetate and acetone fractions were pooled, and careful gradient elution on silica gel (4.5 × 40 cm) with ethyl acetate and acetone gave 500 mg of a viscous oil possessing toxicity.

The clear oil contained no UV-absorbing chromophore. Mass spectrometric analyses, CI MS negative ion (N_2O), *m/z* 229 $(M - H)^-$, and positive ion (CH_4), *m/z* 213 $(M + H - H_2O)^+$, suggested a molecular formula of $C_{12}H_{22}O_4$ (*m/z* 213.1484, $C_{12}H_{21}O_3$ calcd 213.1491).[4] ^1H NMR (360 MHz, $CDCl_3$) measurements (ordinate of Figure 1) revealed an integrated proton intensity roughly twice that suggested by MS and rigorous chromatographic analysis on radial compression HPLC (10 μm of Si with $CHCl_3$/1% MeOH) suggested that the sample was isolated as an equal mixture of two components. Because a large-scale separation

(1) Bragman, H. H.; Dickey, H. C.; Plummer, B. E.; Poulton, B. R. *J. Anim. Sci.* **1964**, *23*, 869.

(2) Bhattacharya, A. N.; Fontenot, J. P. *J. Anim. Sci.* **1966**, *25*, 367–371.

(3) Kerksey, J. W.; Cole, R. J. *Mycopathol. Mycol. Appl.* **1974**, *54*, 291–294.

(4) Chemical ionization mass spectral data obtained on a Finnigan 3200 quadrupole mass spectrometer and high-resolution data obtained on a VG-770 at Harvey Laboratories, Inc.

0002-7863/82/1504-7319$01.25/0

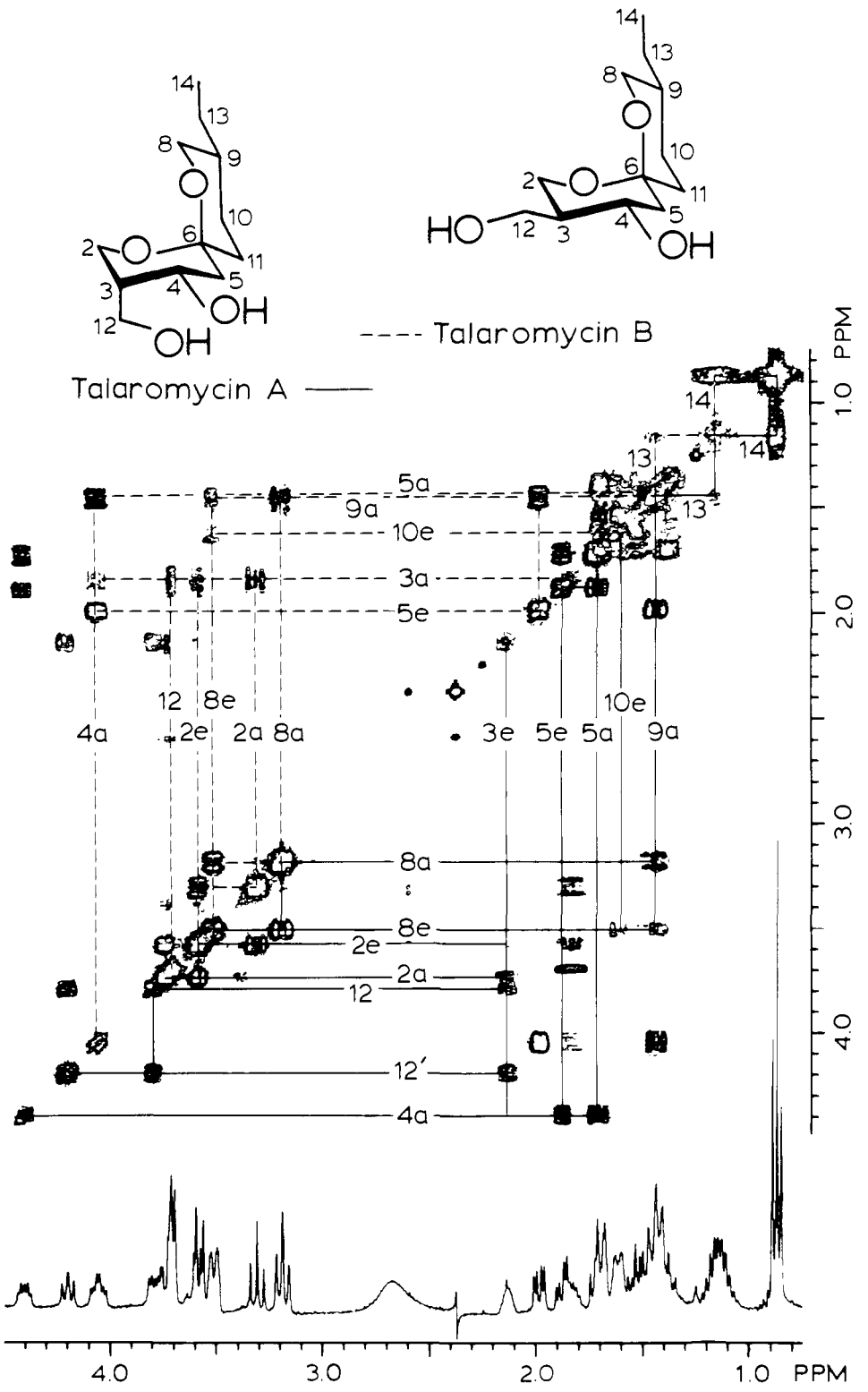

Figure 1. Contour plot of the 360-MHz[19] homonuclear spin correlation map of the mixture of the two diastereomeric talaromycins. The two-dimensional map is composed of 256–512 data point spectra, each incremented by 568 μs. A 15-s delay was allowed between each pulse sequence. The data were acquired with quadrature phase detection in both dimensions, and the final data were symmetrized.[20] Although the cross peaks are symmetrical across the diagonal, the lines placed on the spectrum connect each isomer individually. The intensity of the cross peaks has been found to vary, and although the cross peak between H_{3e} and H_{4a} does not appear for talaromycin A, lower slices as well as a stacked plot of the data confirm its presence. The processing and plotting of this data took ca. 30 min. The signal at δ 2.37 is $CHCl_3$ folding back into the spectrum, and the broad signal at δ 2.67 is hydroxyl protons.

of the components was not feasible, two-dimensional ^{1}H NMR correlation spectroscopy was chosen as an attractive method for analysis of the mixture.[5]

Utilization of the pulse sequence first explored by Jeener[6] and later extended by others[7] generated the 2-D data set in Figure

(5) Van Divender, J. M.; Hutton, W. C. *J. Magn. Reson.* **1982**, *48*, 272–279.

(6) Jeener, J. Ampere International Summer School, Basko Polje, Yugoslavia 1971, unpublished material.

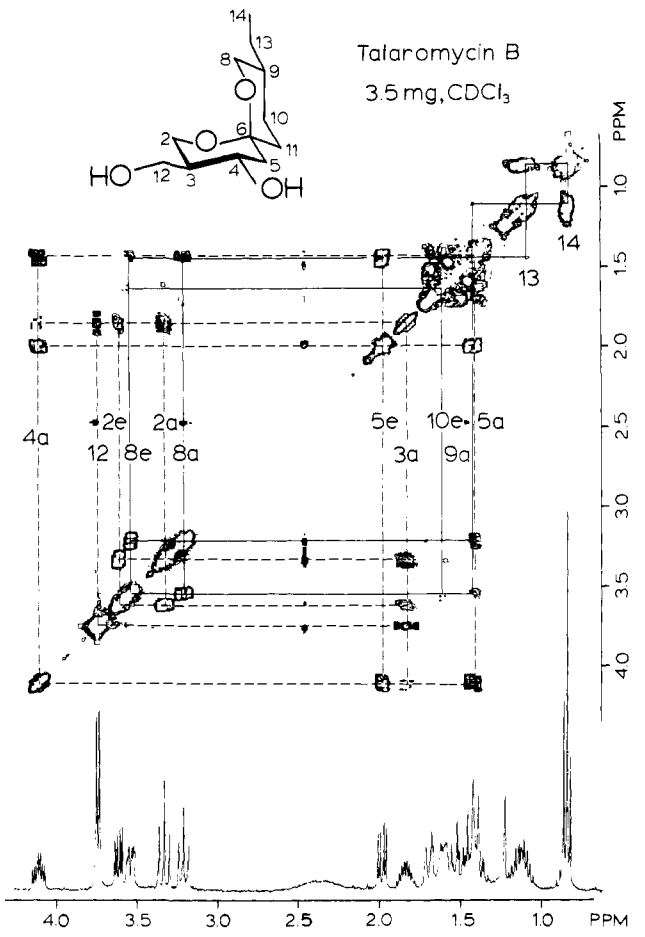

Figure 2. The two-dimensional map is composed of 128–512 data point spectra, each incremented by 555 μs. A 5-s delay was allowed between each pulse sequence, giving a total accumulation time of 2.49 h. The data were acquired with quadrature phase detection in both dimensions, and the final data were zero filled in the F_1 dimension and symmetrized. The cross peaks are connected on both sides of the diagonal, and the proton assignments are indicated. An impurity is present at δ 1.28.

1. The diagonal signals, with identical chemical shift on both axes, are present for every signal in the 1-D spectrum. The off-diagonal contour intensity arises from magnetization transfer through spin–spin relaxation of coupled spin systems. The identification of these off-diagonal signals allows for the establishment of all J coupling connectivities. The identification of independent, isolated spin systems possessing a large degree of similarity, as indicated in Figure 1, suggested that the mixture was composed of structurally related components. The symmetry of the proton-coupling patterns and the MS identification of half the number of protons seen in ^{1}H NMR supported the assignment of these components as stereoisomers.

Deuterium-exchange negative ion CI MS (CH_3OD, N_2O),[8] m/z 230 $(M - 1)^-$ with one exchange, identified two exchangeable protons. Formation of the phenyl boronic ester[9] ($C_6H_5B(OH)_2$ benzene, Dean Stark) confirmed the presence of two hydroxyl groups. Esterification with the UV-visible phenylboronic acid also rendered the previously unresolvable isomers chromatographically separable (PTLC, $CHCl_3$, 5×). Quantitative removal of the phenylboronic acid (ether, dilute NaOH) yielded the purified talaromycins A and B.

(7) Aue, W. P.; Bartoldi, E.; Ernst, R. R. *J. Chem. Phys.* **1976**, *64*, 2229–2246. Nagayama, K.; Wuthrich, K.; Ernst, R. R. *Biochem. Biophys. Res. Commun.* **1979**, *90*, 305–311. Bax, A.; Freeman, R.; Morris, G. *J. Magn. Reson.* **1981**, *42*, 164–168. Bax, A.; Freeman, R. *J. Magn. Reson.* **1981**, *44*, 542–561.

(8) Hunt, D. F.; Sethi, S. K. *J. Am. Chem. Soc.* **1980**, *102*, 6953–6963. Lynn, D. G.; Steffens, J. C.; Kamat, V. S.; Graden, D. W.; Shabanowitz, J.; Riopel, J. L. *Ibid.* **1981**, *103*, 1868–1870.

(9) Ferrier, R. J. *Adv. Carbohydr. Chem. Biochem.* **1978**, *35*, 31–80.

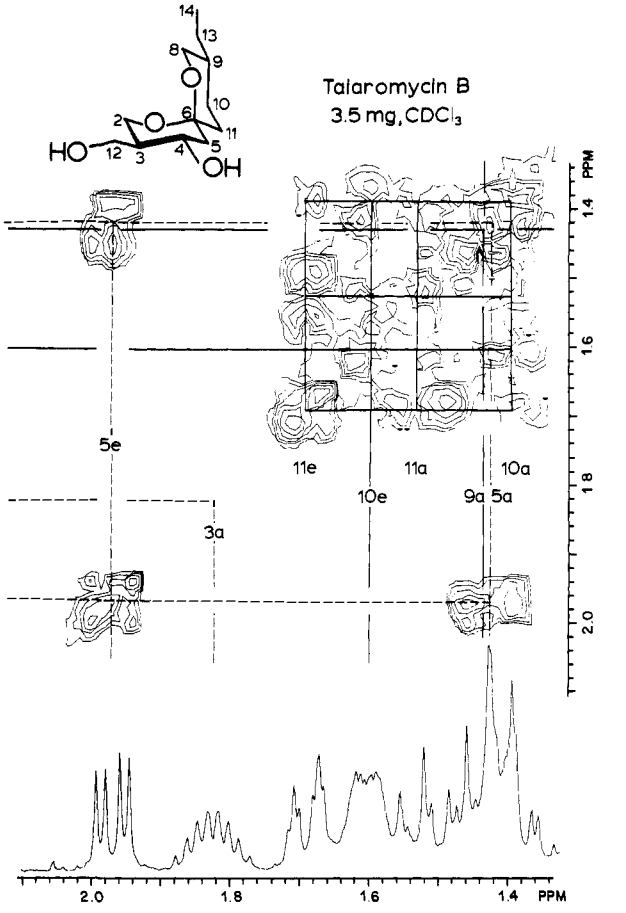

Figure 3. Expansion of the high-field region of the talaromycin B spectrum in Figure 2. The solid and dashed lines here and in Figure 2 distinguish the two isolated spin systems of talaromycin B.

Hydroxyl proton coupling, observed in the purified talaromycin samples lacking prior D_2O exchange, identified the protons α to the OH groups. With this assignment providing a point of orientation, the spin correlation map of each isomer (Figure 2) established the adjacent spin-coupled protons sequentially in a manner similar to a series of decoupling experiments. The advantage of the COSY experiment is seen in the assignment of the congested high-field region of talaromycin B (Figure 3). The relative stereochemistries of the substituents were assigned by the magnitude of the coupling constants,[10] and while this information is not quantitatively obtained in the Jeener map, qualitative information is available from the intensity of the off-diagonal signals (see H_{2e} vs. H_{2a} coupling to H_{3a}, Figure 2). The stereochemical difference between the talaromycins is apparent in the *trans*-diaxial coupling between H_{3a} and the adjacent H_{2a} and H_{4a} in talaromycin B (11 Hz) and the smaller couplings observed for H_{3e} in talaromycin A (2.8 and 5.4 Hz, respectively). This coupling difference is also apparent in the intensity of the off-diagonal peaks between these same protons in Figure 1.

The spin correlation maps of each of the talaromycins identified two isolated spin-coupling systems (Figures 2 and 3). The ^{13}C NMR (50.3 MHz, $CDCl_3$) of the mixed sample gave a single

(10) Talaromycin A: 360 MHz ^{1}H NMR ($CDCl_3$) δ 3.73 (H_{2a}, dd, J = 11, 2.8 Hz), 3.56 (H_{2e}, dd, J = 11, 1.4 Hz), 2.12 (H_{3e}, m), 4.39 (H_{4a}, ddd, J = 11, 5.1, 5.4 Hz), 1.70 (H_{5a}, dd, J = 13, 11 Hz), 1.87 (H_{5e}, dd, J = 13, 5.1 Hz), 3.17 (H_{8a}, t, J = 11 Hz), 3.50 (H_{8e}, dm), 1.43 (H_{9a}, m), 1.35 (H_{10a}, dq, J = 13, 3.8 Hz), 1.60 (H_{10e}, dm), 1.49 (H_{11a}, dt, J = 13, 4.2 Hz), 1.67 (H_{11e}, dm), 4.18 (H_{12}', dd, J = 11, 9.0 Hz), 3.78 (H_{12}, dd, J = 11, 5.0 Hz), 1.13 (H_{13}, 2 H, m), 0.85 (H_{14}, 3 H, t, J = 7.8 Hz). Talaromycin B: 360 MHz ^{1}H NMR ($CDCl_3$) δ 3.28 (H_{2a}, t, J = 11 Hz), 3.56 (H_{2e}, dd, J = 11, 4.6 Hz), 1.82 (H_{3a}, m), 4.04 (H_{4a}, dt, J = 11, 5.1 Hz), 1.42 (H_{5a}, dd, J = 12, 11 Hz), 1.97 (H_{5e}, dd, J = 12, 5.1 Hz), 3.17 (H_{8a}, t, J = 11 Hz), 3.49 (H_{8e}, dm), 1.43 (H_{9a}, m), 1.38 (H_{10a}, dq, J = 13, 3.6 Hz), 1.60 (H_{10e}, dm), 1.52 (H_{11a}, dt, J = 13, 4.0 Hz), 1.68 (H_{11e}, dm), 3.68 (H_{12}, 2 H, d, J = 6.0 Hz), 1.13 (H_{13}, 2 H, m), 0.85 (H_{14}, 3 H, t, J = 7.5 Hz).

low-field resonance, δ 97.2, suggestive of equivalent ketal centers in each isomer.[11] Acid-catalyzed equilibration (0.1 N *p*-TSA in THF, room temperature) of talaromycin A (0.5 mg) quantitatively converted the less-stable axial hydroxymethylene isomer into talaromycin B and thus proved the presence of the ketal functionality.[12] The ketal's relative configuration[13] was established by observing the nuclear Overhauser enhancement of H_{2a} (3.7%)[14] on irradiation of H_{8a} in talaromycin A. Similar irradiation of H_{2a} in **1** gave enhancements of H_{2e} (15%), H_{3e} (6.3%), H_{4a} (2.3%),

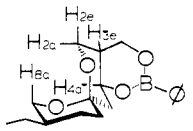

1

and also H_{8a} (4.0%).[15] These enhancements verified the ring conformations shown in **1** and also established the three-dimensional positions of H_{8a} and H_{2a}, two protons that would be proximal only if both oxygens occupied axial positions in the spiro-fused ketal.

The structural characterization of the talaromycins has shown COSY to be a powerful method for resolving isomeric mixtures (Figure 1) and for identifying spin systems isolated by regions devoid of protons (Figures 2 and 3). Even though this experiment gives comparable data to a series of double resonance experiments, the opportunity to obtain all the information in a single experiment, even in highly congested regions where decoupling is difficult, provided an important advantage in the talaromycin assignment. This ability to verify all the proton-coupling connectivities of a molecular structure allows for a formal assignment of all the protons and leads to a nonempirical establishment of structure.

The spiro ketal present in the talaromycins is a structural feature common to many bacterial polyether antibiotics[16] as well as to several insect pheromones.[17] The talaromycins constitute the first example of such functionality being elaborated in fungi through what appears to be a polyketide pathway. The toxicity of the talaromycins is still under investigation, but initial data suggest that they block outward potassium fluxes and thus lead to muscle dysfunction.[18]

Acknowledgment. The funds for the purchase of the NTC 360 spectrometer were partially provided by NSF. We thank Research Corp. for partial support, Professor Steven Weinreb, Pennsylvania State University, for obtaining the ^{13}C NMR of the mixed sample, and Dr. Jerry Golik and Professor Koji Nakanishi, Columbia University, for helping to obtain and interpret the CD spectra of the benzoates of the talaromycins.

(11) The ^{13}C chemical shift of the spiro ketal carbon does not appear to have any predictive value as to configuration, but the thermodynamic stability of such systems has been explored: Pothier, N.; Rowan, D. D.; Deslongchamps, P.; Saunders, J. K. *Can. J. Chem.* **1981**, *59*, 1132-1139. Francke, W.; Reith, W.; Sinnwell, V. *Chem. Ber.* **1980**, *113*, 2686-2693.

(12) Opening of the ketal results in two equivalent primary alcohols that will close to the thermodynamically most stable isomer. At this point we have no direct data as to whether only one isomer is naturally occurring and the second is a function of our isolation procedure, but we suspect that both isomers occur naturally.

(13) CD analysis of the dibenzoates (benzoyl chloride, pyridine) of the talaromycins has indicated that the absolute configuration indicated in **1** is correct.

(14) Preirradiation (selective 180°) of the desired signal in talaromycin A (1.5 mg in 0.5 mL $CDCl_3$) was followed after a delay (0.7 s) by a 90° observed pulse. This spectrum (500-1000 transients) was acquired simultaneously with a spectrum where the selective pulse was applied 3 ppm upfield of Me_4Si, and the two spectra were computer subtracted to observe the enhancements: Solomon, I. S. *Phys. Rev.* **1955**, *99*, 559-565. Hall, L. D.; Sanders, J. K. M. *J. Chem. Soc., Chem. Commun.* **1980**, 368-370.

(15) The phenyl boronic esters, **1**, were more easily dried and provided better observation of small NOE. The small chemical shift difference between H_{2a} and H_{8a} in talaromycin B did not allow for quantitative measurements of the NOE's.

(16) Westley, J. W. *Adv. Appl. Microbiol.* **1977**, *22*, 177-222. Westley, J. W. "The Polyether Antibiotics: Carboxylic Acid Ionophores"; Westley, J. W., Ed.; Marcel Dekker: New York, 1982: Chapter 1.

(17) Baker, R.; Herbert, R.; Howse, P. E.; Jones, O. T.; Francke, W.; Reith, W. *J. Chem. Soc., Chem. Commun.* **1980**, 52-53. Francke, W.; Reith, W.; Bergström, G.; Tengö, J. *Naturwissenschaften* **1980**, *67*, 149-150. Baker, R.; Herbert, R. H.; Parton, A. H. *J. Chem. Soc., Chem. Commun.* **1982**, 601-603.

(18) The molecular action of the talaromycins is still under investigation by Dr. Stuart Taylor, Department of Pharmacology, The Mayo Foundation, Rochester, MN.

(19) ^1H NMR data obtained with an NTC-360 spectrometer with a 1280/293B data system and standard NMCFT software.

(20) Baumann, R.; Wider, G.; Ernst, R. R.; Wüthrich, K. *J. Magn. Reson.* **1981**, *44*, 402-406.

Transient Raman Scattering Observation of Surface Reactions in Aqueous TiO_2 Colloids

R. Rossetti, S. M. Beck, and L. E. Brus*

Bell Laboratories, Murray Hill, New Jersey 07974

Received August 30, 1982

Absorption of light by semiconductor particles in an aqueous colloid creates mobile electrons (e^-) and holes (h^+) that may migrate to the particle surface and undergo redox processes with adsorbed chemical species. Both e^- and h^+ come to the surface apparently because the particle dimensions are small with respect to the characteristic band-bending length. The optimization and mechanism of such reactions have been intensively studied in recent years, principally by using transient absorption spectroscopy of the reaction products.[1-7] We, as well as others, have recently discovered that the kinetics of the reaction precursor species e^- and h^+ can be observed via radiative recombination emission.[8-9]

Transient Raman scattering analysis of chemical reactions provides direct structural information about reactive intermediates. In addition, variations in the local molecular environment of a given species are sometimes observed as small shifts in the spectra, for example, in heme proteins[10] and on the hydrocarbon:water boundary in aqueous micelles.[11] We now report application of this technique to semiconductor surface redox processes in aqueous colloids.

In our experiment e^- and h^+ are created by absorption of an ultraviolet laser pulse at a frequency above the semiconductor band gap ($\lambda \leq 3800$ Å for TiO_2). After a time delay Δt a Raman spectrum is generated by a second pulse at a frequency below the band gap. The semiconductor is transparent at the Raman probe wavelength, which is chosen to give electronic resonance Raman enhancement for a specific chemical species. In this respect, our experiment differs from recent observations of enhanced Raman scattering by stable, transparent species in absorbing metal colloids.[12-14] Our apparatus has been described recently.[15]

(1) Inone, T.; Fujishima, A.; Konishi, S.; Honda, K. *Nature (London)* **1979**, *277*, 637.

(2) Kraentler, B.; Bard, A. J. *J. Am. Chem. Soc.* **1978**, *100*, 5985.

(3) Borgarello, E.; Kiwi, J.; Pelizzetti, E.; Visca, M.; Grätzel, M. *Nature (London)* **1981**, *289*, 159.

(4) Kalyanasundaram, K.; Borgarello, E.; Duonghong, D.; Grätzel, M. *Angew. Chem., Int. Ed. Engl.* **1981**, *20*, 987.

(5) Fujihira, M.; Satoh, Y.; Osa, T. *Nature (London)* **1981**, *293*, 206.

(6) Humphry-Baker, R.; Lilie, J.; Grätzel, M. *J. Am. Chem. Soc.* **1982**, *104*, 422.

(7) Duonghong, D.; Ramsden, J.; Grätzel, M. *J. Am. Chem. Soc.* **1982**, *104*, 2977. We thank Professor Grätzel for a preprint of this paper.

(8) Rossetti, R.; Brus, L. E. *J. Phys. Chem.* **1982**, *86*, 4470.

(9) Henglein, A. *Ber. Bunsenges. Phys. Chem.* **1982**, *86*, 241.

(10) Lyons, K. B.; Friedman, J. M.; Fleury, P. A. *Nature (London)* **1978**, *275*, 565.

(11) Beck, S. M.; Brus, L. E. *J. Am. Chem. Soc*, in press.

(12) von Raben, K. U.; Chang, R. K.; Laube, B. L. *Chem. Phys. Lett.* **1981**, *79*, 465.

(13) Creighton, J. A.; Blatchford, C. G.; Albrecht, M. G. *J. Chem. Soc., Faraday Trans. 2* **1979**, *75*, 790.

(14) Kerker, M.; Siiman, O.; Bumm, L. A.; Wang, D. S. *App. Optics* **1980**, *19*, 3253.

(15) Beck, S. M.; Brus, L. E. *J. Chem. Phys.* **1981**, *75*, 4934.

0002-7863/82/1504-7322$01.25/0